Shape optimization for improved understanding of magmatic plumbing systems

Théo Perrot, Freysteinn Sigmundsson

June 2024

Abstract

Inverse problems in volcanic geodesy are crucial for identifying the location and shape of magmatic bodies based on ground deformation data. Traditional approaches often rely on models with predefined shapes, which can limit their accuracy. To address this, we present a shape optimisation method using a level-set approach that flexibly determines the optimal shape of a magma chamber without prior shape assumptions. By minimising the discrepancy between observed and modelled surface displacements, our adapted algorithm becomes suitable for solving inverse volcano deformation problems. We explore the capabilities of this approach with synthetic data and apply it to InSAR observations of the Svartsengi volcanic system in Iceland, demonstrating its potential to improve volcanic hazard assessment after maturation through future work.

1 Introduction

1.1 Challenge

In volcano geodesy, inverse problems are central to estimating the position of magmatic bodies using ground motion as a proxy. Displacement is observed by geodetic measurements such as Global Navigation Satellite System (GNSS) point positioning, leveling campaigns, or Synthetic Aperture Radar (InSAR) interferometry within a volcanic field, and the subsurface processes causing the movement are inferred from these observations (Dzurisin 2007). Magmatic sources are modeled as pressurized cavities that deform the surrounding host rocks and cause the surface to move. Various inversion methods based on parametric analytical or numerical models aim at finding the optimal values for the vector of d free parameters $\vec{m} \in \mathbb{R}^d$ of the model. Then an error function $J(\vec{m})$ is representative of the misfit between the observed displacements and the prediction of the model. $\vec{m}_{opt}$ can then be found using various inversion techniques that minimize J: global optimization based on analytic (Cervelli et al. 2001) or numerical models (Hickey and Gottsmann 2014, Charco and Galán del Sastre 2014), Bayesian inference (Bagnardi and Hooper 2018, Trasatti 2022), or genetic algorithms (Velez et al. 2011) on analytic models. The choice of the method is constrained by the reasonable number of evaluations of $J(\vec{m})$: numerical models handle a complex description of the system, but are computationally expensive compared to analytic models, which on the other hand may lead to an oversimplification (Taylor, Johnson, and Herd 2021).

However, each of these finite-dimensional optimization methods is limited by the intrinsic assumption of a definite parametric shape for the source. In fact, analytic expressions can be derived for only a few regular shapes such as point source (Mogi 1958), finite sphere source (McTigue 1987), or ellipsoidal source (Yang, Davis, and Dieterich 1988), and any numerically generated shape must be parameterized to be inverted. Even in the case where complex shapes are chosen, they would require additional describing parameters, and ultimately any of the above methods may face the curse of dimensionality. The goal of this paper is not to give a definitive answer to these limitations, but rather to lay the first stone for a new approach that overcomes these difficulties.

1.2 Shape optimization

Shape (and topology) optimization aims to find the shape that minimizes a given function defined on a given system, without the need for prior assumptions about shape and topology. It is actively developed by part of the applied mathematics community and is widely used in engineering to find optimal designs for systems: In structural mechanics, to maximize the stiffness of a solid structure such as a cantilever beam (Bendsøe and Ole Sigmund 2004), in fluid-structure interaction on heat exchangers or flying obstacles (F. Feppon et al. 2020), and even as a way to explore new architecture for buildings (Beghini et al. 2014). Most finite element simulation and design software now implements an embedded shape optimization module (Frei 2015, Slavov and Konsulova-Bakalova 2019, Le Quilliec 2014). However, its use has not yet been reported in the context of inverse problems in volcano geodesy, where it can overcome the shape hypothesis problem as long as an internal pressure value is assumed.

Many paradigms coexist in shape optimization as reviewed by Ole Sigmund and Maute 2013, one of the most popular being SIMP optimization, where a density value is optimized for each element of the mesh with values between 0 (void) and 1 (material) before being black and white filtered to output a design (O. Sigmund 2001,Bendsøe and Ole Sigmund 2004), with several open source implementations (Andreassen et al. 2011,Hunter et al. 2017). We chose level-set shape optimization instead because it has the advantage of providing an explicit representation of the boundary at each step of the optimization, which is crucial for us as explained later (section 2). For this, we relied on the work of Dapogny and Florian Feppon 2023, who thoroughly described and vulgarized the method, as well as providing a freely available open source implementation of the method, `sotuto`(Dapogny and Florian Feppon 2024), which we modified and extended to adapt it to inverse geodetic problems.

2 Method

Here we briefly present the key ingredients of level set shape optimization along with their implications for our problem. The full mathematical background on which it relies is not detailed, but see this chapter by Allaire, Dapogny, and Jouve 2021 for a comprehensive step-by-step description supported by proofs and theorems. It is also worth noting that many aspects of secondary importance to the method are not mentioned for the sake of brevity. For the unfamiliar reader interested in understanding the method, the lecture (especially part III) given by Dapogny and Bonnetier 2024 at the Université Grenoble Alpes is also recommended.

2.1 Model

Let Ω be a bounded domain of $\mathbb{R}^3$ whose shape we want to optimize by modifying parts of its boundary $\partial\Omega$. As for classical analytical models of volcanic deformation induced by magmatic activity, Ω is a domain representing a portion of the shallow Earth crust, including the volcano, assumed to be homogeneous, isotropic, and elastic. The governing equations are $-div(Ae(u)) = 0$ in Ω, where $e(u)$ is the strain tensor of the displacement field u and A is the constitutive law tensor, $Ae = 2\mu e + \lambda tr(e) Id$ for linear elasticity. Boundaries under different conditions, see Fig. 1 for all notations.

The part of $\partial\Omega$ to be optimized is Γ_s, the boundary of magma chamber, which is modeled as an empty, uniformly pressurized cavity. Therefore, a value for the internal pressure ΔP must be assumed (see Discussion for development). In the following text we talk about optimizing $\partial\Omega$, but in practice only $\Gamma_s \subset \partial\Omega$ is of interest and will be modified, any other boundary will be fixed during the iterations.

We want to find $\partial\Omega$ such that the displacement of the model $u(\Omega)$ is as close as possible to the observed displacement u_o on the surface Γ_u. Thus, the unconstrained shape optimization problem we want to solve is the minimization of a squared RMS discrepancy

$$\min_{\Omega} J(\Omega) = \int_{\Gamma_u} (u(\Omega) - u_o)^2 dS \tag{1}$$

2.2 Hadamard Boundary Variation

Overall, this method can be considered a classical iterative gradient descent algorithm. J is first initialized at J_0 with an instructed first guess for Ω_0 and then iteratively decreased by moving $\partial\Omega$ of a given step in a given descent direction $\theta : \mathbb{R}^3 \mapsto \mathbb{R}^3 \in W^{1,\infty}$ (the Sobolev space of uniformly bounded functions, Allaire, Dapogny, and Jouve 2021) chosen using the shape derivative $J'(\Omega)(\theta)$.

The boundary variation method of Hadamard 1908 introduces the notion of shape differentiation $F'(\Omega)(\theta)$ of a functional F defined on Ω in the direction θ. In short, such a derivative is based on the variation of a bounded domain $\Omega \mapsto \Omega_\theta := (Id + \theta)(\Omega)$: the surface $\partial\Omega$ is slightly moved according to a small vector field $\theta(x)$, as shown in Fig. 2. Once such a derivative exists, one can compute a descending direction at the nthstep θ_n, such as $J'(\Omega)(\theta_n) \leq 0$, so $J_{n+1} \leq J_n$, to decrease the value of J at each iteration.

In our case, after derivation based on the Cea 1986 formal method, we

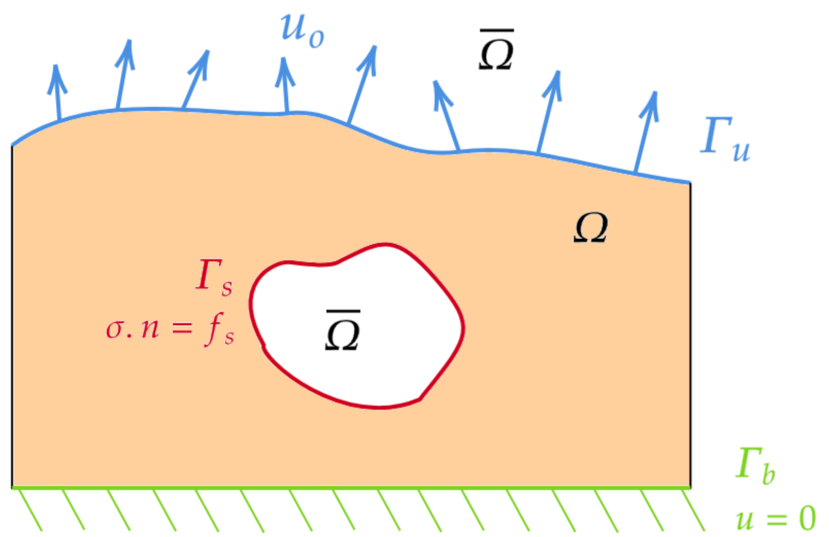

Figure 1: 2D sketch of the problem. The optimized boundary (where the level-set function is zero) is the magma chamber wall Γ_s subjected to a uniform normal load $\sigma(u).n = f_s$ on Γ_s, where $f_s = -\Delta P.n$, where n is the unit normal vector and ΔP is the pressure change between the magma source and the surrounding crust. The bottom surface Γ_b is fixed ($u = 0$). The other boundaries are free. The target displacement field u_o is known on the upper surface Γ_u.

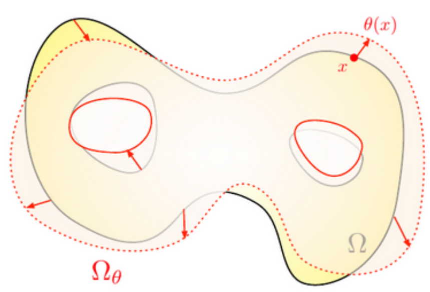

Figure 2: Reproduced from Allaire, Dapogny, and Jouve 2021

found under the variational form :

$$J'(\Omega)(\theta) = \int_{\Gamma_s} \left(Ae(u) : e(p) + \frac{\partial f_s}{\partial n} p + \frac{\partial p}{\partial n} f_s + \kappa f_s p \right) .\theta.ndS \qquad (2)$$

where $\kappa = div(n)$ is the mean curvature at the boundary, and p is the adjoint solution of

$$\forall v \in H^1(\mathbb{R}^3), \int_{\Gamma_u} 2(u_\Omega - u_o)v dS + \int_\Omega Ae(v) : e(p)dV = 0 \qquad (3)$$
$$\text{and } p = 0 \text{ on } \Gamma_b$$

From there, we can trivially move Ω in the direction $\theta = -A$ (where A is the integrand term in parentheses) to ensure that $J'(\Omega)(\theta) \leq 0$. This guarantees that $J(\Omega_{n+1}) \leq J(\Omega_n)$: the series $J(\Omega_n)$ converges to a minimum.

2.3 Level-set representation

A key issue is the representation of the surface to be optimized. The level set method allows to track dramatic changes as well as topology variations (creation of new holes). A certain function $\phi : D \mapsto \mathbb{R}$ is defined over the domain $D \in \mathbb{R}^3$ in such a way that the shape boundary is the level set 0, i.e. reads $\partial\Omega = \phi(x = 0)$. Basically, ϕ can be taken as the signed distance between any point x and $\partial\Omega$, as shown in the example fig. 3. In this way, $\partial\Omega$ is implicitly manipulated when transforming ϕ.

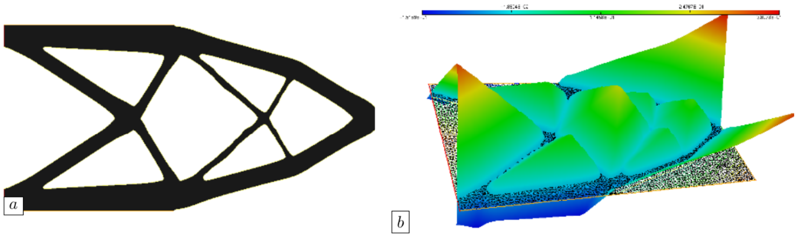

Figure 3: Reproduced from Dapogny and Florian Feppon 2023

Ω_n is then deformed by advecting the corresponding ϕ_n with a velocity field $V(x) = \tau_n\theta_n$, where τ_n is the additional step size. The advection equation usually appears in fluid mechanics to describe the evolution of a quantity transported by a given velocity field, but here there is a smooth and flexible way to modify ϕ which ensures smoothness of Ω_{n+1} and change of topology (see Allaire, Dapogny, and Jouve 2021).

2.4 Numerical implementation

2.5 Numerical implementation

In practice, the D domain is discretized into a mesh T_n on which each variational form is solved at each iteration n. This includes the solution of the elasticity to get u_n, the adjoint state p_n, the computation of the shape gradient J'_n, the descent direction θ_n, the advection of ϕ_n. In `sotuto` it is achieved by calling scripts written in FreeFem++, a finite element software that allows solving any integral form of elliptic PDE (Hecht 2012).

Once the new form Ω_{n+1} is computed and discretized thanks to a local remeshing phase, a new evaluation of J^{n+1} is performed. Since τ is arbitrarily fixed and initialized to 1, it can happen that Ω_n is shifted by too large a step and so $J_{n+1} is \geq J_n$. To adjust the step size, a line search procedure is implemented and adjusts the step size by decreasing it if the new iteration is the worst to ensure an improvement of J by computing a new Ω_{n+1} being a less deformed version of Ω_n. On the contrary, if Ω_{n+1} is accepted, τ is increased to speed up convergence. A tolerance is set to accept iterations if the increase in J is reasonable.

The global optimization loop has no termination criterion. Thus, it is up to the user to stop it when no significant improvement in J can be achieved, or when the shape is not realistic.

The loop and the line search are implemented in Python in `sotuto`. Then the FreeFem scripts are called by the Python script core and data is exchanged via temporary files.

The above aspects are implemented in `sotuto`. However, we extended its functionality to handle our geophysical problem, in a fork we called `magmaOpt`. This included: scripts to create the domain and initial source with GMSH Geuzaine, Remacle, and Dular 2009 ,adapting FreeFem scripts to different error functions, allowing optimization of the loaded boundary Γ_s and so on.

3 Validation with synthetic data

To test the method, the idea is to do a kind of cross-validation. On the one hand, the observation data is a synthetic 3D displacement field for which we know the source parameter. On the other hand, we initialize the algorithm with a first guess for the source shape and location. We expect the algorithm to iteratively modify the shape of the source and converge to the correct shape and location. In fact, the 3D location of the source (e.g., its center of gravity for a random shape) is not directly optimized as a vector of discrete parameters, but is modified by the simple fact that the boundary is free to move in any direction, and thus can take on a kind of "average rigid body motion" as it gradually moves the center in a given direction.

In practice, the synthetic observed surface displacement field is derived from the Mc Tigue solution, an analytical approximation of the displacement caused by a uniformly pressurized spherical cavity (the magma domain) embedded in an isotropic, homogeneous, and planar elastic medium (the host crust) McTigue 1987 with elastic constants tp $E = 10\text{GPa}$ and $\mu = 0.25$.

Usually, the quantities to be determined with parametric inversion based on a McTigue model are the location and the radius. The pressure change can also be left as a free parameter, but is interchangeable with the radius, so one must be fixed to determine the other, see (Greiner 2021) for more details. For the synthetic source, we fixed these free parameters to $z = -5\text{km}$, $\Delta P = 10\text{MPa}$, $R = 1.5\text{km}$, which are typical values for inverted magmatic domains.

On the other hand, to test the robustness of the method, we tried different initial Ω_0 shapes. The tests included: same center but different shape, different center but same shape, and different shape and center, as summarized in the table **??**.

`magmaOpt` is then allowed to run freely, without any termination condition, to see whether or not it succeeds in converging from the ellipsoid to the McTigue sphere we used to generate the synthetic displacement.

Since there is no termination condition here, we take the shape corresponding to the smallest value of J found as the best result (although it can be discussed, see the conclusion). To evaluate the quality of the result, we use two different metrics. On the one hand, the distance between the centroids of the final source and the synthetic sphere is an indicator of the distance between the two corps and assesses whether the final shape taken as a rigid body is overall correctly located. On the other hand, after aligning the final source surface on the sphere using an iterative point cloud (ICP) algorithm, we use the chamfer distance to asses the difference in terms of shape.

4 Real test case : Svartsengi 2022 inflation

We now apply the method to infer the shape of a magma domain in a recent period of volcanic unrest and eruption in SW Iceland by evaluating the shape of a magma body responsible for the ground inflation observed from 21 April to 14 June 2022 at Svartsengi on the Reykjanes peninsula. This is one of 5 inflation episodes that preceded catastrophic dike breaches and eruptions at the Sundhnúkur crater row, which caused the destruction of the city of Grindavík (Sigmundsson et al. 2024).

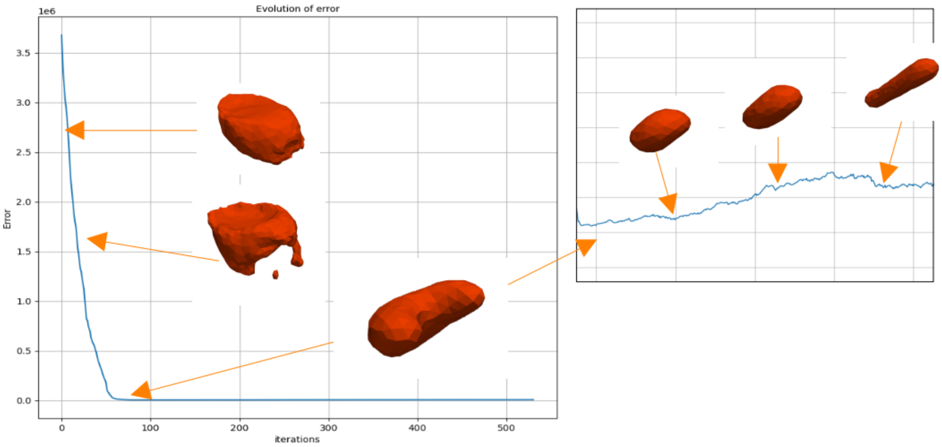

Figure 4: Evolution of error and succesivve shapes taken by the magma source during an optimization loop. The initial guess is a flat ellipsoid of semi-axes $r_x = 2\text{km}, r_y = 3\text{km}, r_z = 1\text{km}$ centered on the true spherical source. The minimum is reached at iteration 82.

The observational data used are the line-of-sight (LOS) displacement maps of the area from Cosmo SkyMed available in Parks et al. 2024, the data used in Sigmundsson et al. 2024. After uniform downsampling and mesh reprojection (the data points must be aligned on the mesh nodes), the ascending A32 and descending D132 tracks were both used in the RMS error function we adapted to the LOS geometry.

$$J(\Omega) = \sum_{i \in tck} \alpha_i \int_{\Gamma_u} \left(L_i(u(x)) - l_o^i(x) \right)^2 dS \tag{4}$$

Where $tck = \{A125, D132\}$. For each track i, α_i is the weight of the track ($\forall i, \alpha_i = 1$ here), $L_i : \mathbb{R}^3 \mapsto \mathbb{R}$ is the function that projects the 3D surface displacement given by the model into the LOS geometry, and l_o^i is the observed LOS displacement.

We then used the framework developed above, only projecting the InSAR data onto the mesh of D and modifying the expression of the error function in `magmaOpt`.

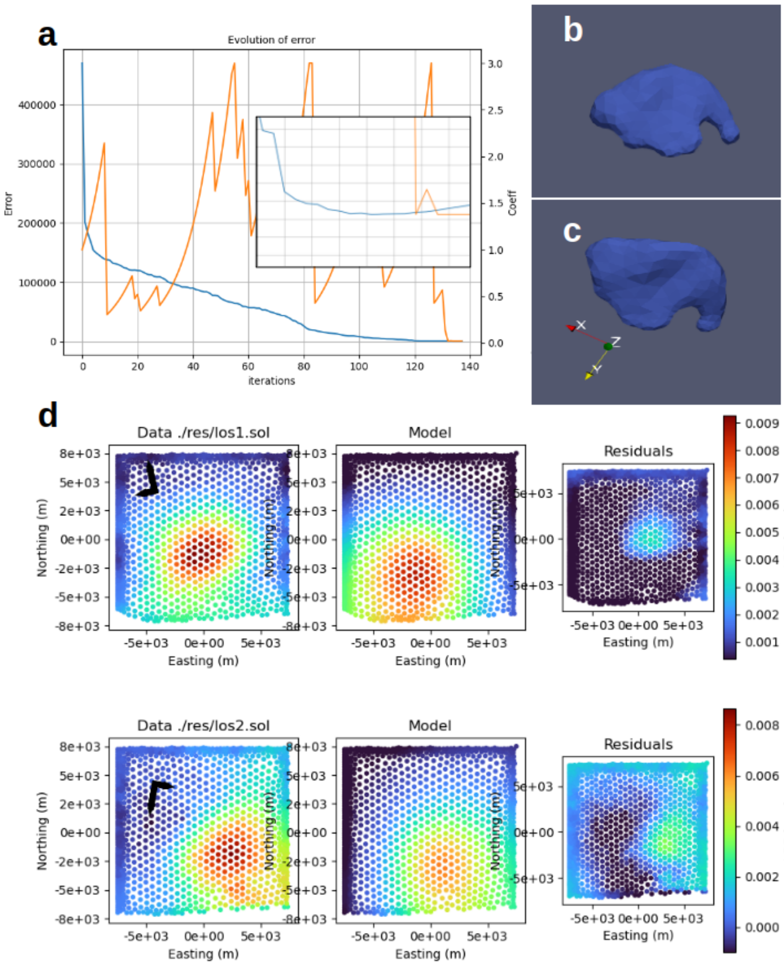

Figure 5: a) Convergence plot with embedded zoom. The blue line is the error and the orange line is the evolution of τ. Minima are reached at iteration 128. b,c) Side and top view of the source Γ_s minimizing J. d) Data, model and residuals of the LOS displacements at iteration 128 for the two InSAR tracks A32 (top) and D132 (bottom). Black arrows are heading and looking directions, coordinates are ISN16 Íslands 2024 shifted to a local origin $(2529373E, 179745N)$.

The results shown in figure 5 are encouraging: after providing an initial guess located at the center of inflation at depth for a sphere of radius RR, the algorithm is able to iteratively change the shape and depth of the magma domain to finally result in a sill-like flattened spheroid whose centroid is located at DD depth. This is consistent with the presumed depth found in the supporting information of Sigmundsson et al. 2024, which performs an analytical model-based inversion. Although the pressure must be fixed, as explained in 1.2, the result can be used to compare the final shape of the magmatic intrusion and give a richer insight into it. Here we see interesting features, such as an increasing thickness on the north side, that can't be traced by any other method. The algorithm produces features that we consider to be artifacts, probably due to mesh refinement problems, such as small holes or horn-shaped features.

5 Discussion

This work paves the way for a new class of methods that tackle an unknown geometry of the magmatic domains, thus giving the possibility to explore irregular shapes that are more likely to exist compared to any other usually assumed regular shapes. However, even if the first results presented are promising, many questions remain to be answered. First of all, the internal pressure of the chamber must be specified, which is a strong hypothesis. In this context, the precise shape of the source should be determined as a second step. The traditional analytical model-based inversion would be run first, giving a pressure and a first educated guess for the position and shape of Ω_0. Then a more realistic shape could be sought with a shape optimization taking the output of the inversion as an initial guess.

Adding constraints may also be an interesting way to explore. For example, the volume of the source could be constrained to be within bounds or even to match a certain value. The implemented shape optimization is certainly able to handle constraints as described by **allaire202**. The physical meaning of the best shape might benefit from a more constrained problem, and the less influencing deeper part of the source might be less random.

To better understand the influence of data partitioning and variablitiy, additional tests could be run with synthetic data. We can think of tests such as masking part of the surface displacement field, introducing noise and parasitic signals, reducing the number of data points, as is often the case in reality with areas of volcanic systems lacking data coverage (glacier, river, lava, forest) and subjected to perturbations (atmospheric distortion, weather).

It is also important to mention that the behavior of the algorithm is influenced by numerous parameters of varying importance, starting from the discretization length (element size) or the domain extent, to the limits of the step size τ, the regularization length, or the number of iterations allowed by the line search. A systematic study of each of these parameters would be beneficial in assessing the quality of the shape inferred.

Exploring a way to quantify the uncertainty of the answer is also crucial. For example, a sensitivity analysis approach could be considered, as well as the inclusion of a probabilistic quantity.

6 Conclusion

The present study has successfully demonstrated the application of inverse problems and computational methods to infer the shape of a magma domain beneath a volcano using ground inflation data from satellite observations. The shape optimization technique used in this research showed a new way to identify the most likely shape of the magma chamber. It was intended as an opening to new methods rather than a complete solution.

We have shown that modifying a shape optimization algorithm to handle geophysical problems is feasible and of interest. Tests on synthetic data showed to some extent the relevance of the approach, although the best sources found exposed the limitations faced by these first attempts of shape optimization for volcano geodesy. The test on real data showed a concrete case of how the method could be used after being more mature.

The perspectives are numerous. The numerical nature of the models allows to easily add complexities to the modeling, such as complex mechanical behavior of the crust (plaxticity, viscoelasticity, poroelsaticity), additional loads (tectonic stress, tidal loads, glacier weights), or inhomogeneities. We hope that the open source code `magmaOpt` developed by us will be modified and extended by future work.

By addressing these limitations and extending this approach, researchers can further improve the accuracy and reliability of magma domain shape inference. Ultimately, the development of more sophisticated models will enable geophysicists to better monitor volcanic activity, predict eruptions, and provide critical support for hazard mitigation strategies.

References

Allaire, Grégoire, Charles Dapogny, and François Jouve (2021). “Chapter 1 - Shape and Topology Optimization”. In: *Geometric Partial Differential Equations - Part II*. Ed. by Andrea Bonito and Ricardo H. Nochetto. Vol. 22. Handbook of Numerical Analysis. Elsevier, pp. 1–132. DOI: 10.1016/bs.hna.2020.10.004. URL: https://www.sciencedirect.com/science/article/pii/S1570865920300181.

Andreassen, Erik et al. (Jan. 2011). "Efficient Topology Optimization in MATLAB Using 88 Lines of Code". In: *Structural and Multidisciplinary Optimization* 43.1, pp. 1–16. ISSN: 1615-147X, 1615-1488. DOI: `10.1007/s00158-010-0594-7`. URL: `http://link.springer.com/10.1007/s00158-010-0594-7` (visited on 08/22/2024).

Bagnardi, Marco and Andrew Hooper (July 2018). "Inversion of Surface Deformation Data for Rapid Estimates of Source Parameters and Uncertainties: A Bayesian Approach". In: *Geochemistry, Geophysics, Geosystems* 19.7, pp. 2194–2211. ISSN: 1525-2027, 1525-2027. DOI: `10.1029/2018GC007585`. URL: `https://agupubs.onlinelibrary.wiley.com/doi/10.1029/2018GC007585` (visited on 02/29/2024).

Beghini, Lauren L. et al. (Feb. 1, 2014). "Connecting Architecture and Engineering through Structural Topology Optimization". In: *Engineering Structures* 59, pp. 716–726. ISSN: 0141-0296. DOI: `10.1016/j.engstruct.2013.10.032`. URL: `https://www.sciencedirect.com/science/article/pii/S0141029613005014` (visited on 08/21/2024).

Bendsøe, Martin P. and Ole Sigmund (2004). "Topology Optimization by Distribution of Isotropic Material". In: *Topology Optimization: Theory, Methods, and Applications*. Ed. by Martin P. Bendsøe and Ole Sigmund. Berlin, Heidelberg: Springer, pp. 1–69. ISBN: 978-3-662-05086-6. DOI: `10.1007/978-3-662-05086-6_1`. URL: `https://doi.org/10.1007/978-3-662-05086-6_1` (visited on 08/21/2024).

Cea, Jean (1986). "Conception Optimale Ou Identification de Formes, Calcul Rapide de La Dérivée Directionnelle de La Fonction Coût". In: *ESAIM: Modélisation mathématique et analyse numérique* 20.3, pp. 371–402. ISSN: 1290-3841. URL: `http://www.numdam.org/item/M2AN_1986__20_3_371_0/` (visited on 08/22/2024).

Cervelli, P. et al. (2001). "Estimating Source Parameters from Deformation Data, with an Application to the March 1997 Earthquake Swarm off the Izu Peninsula, Japan". In: *Journal of Geophysical Research: Solid Earth* 106.B6, pp. 11217–11237. ISSN: 2156-2202. DOI: `10.1029/2000JB900399`. URL: `https://onlinelibrary.wiley.com/doi/abs/10.1029/2000JB900399` (visited on 08/22/2024).

Charco, M. and P. Galán del Sastre (Mar. 1, 2014). "Efficient Inversion of Three-Dimensional Finite Element Models of Volcano Deformation". In: *Geophysical Journal International* 196.3, pp. 1441–1454. ISSN: 0956-540X. DOI: `10.1093/gji/ggt490`. URL: `https://doi.org/10.1093/gji/ggt490` (visited on 08/22/2024).

Dapogny, Charles and Eric Bonnetier (2024). *An Introduction to Shape and Topology Optimization*. URL: `https://membres-ljk.imag.fr/Charles.Dapogny/coursoptim.html` (visited on 08/21/2024).

Dapogny, Charles and Florian Feppon (Oct. 31, 2023). "Shape Optimization Using a Level Set Based Mesh Evolution Method: An Overview and Tutorial". In: *Comptes Rendus. Mathématique* 361.G8, pp. 1267–1332. ISSN: 1778-3569. DOI: 10.5802/crmath.498. URL: https://comptes-rendus.academie-sciences.fr/mathematique/articles/10.5802/crmath.498/ (visited on 08/02/2024).

— (July 30, 2024). *Dapogny/Sotuto*. URL: https://github.com/dapogny/sotuto (visited on 08/21/2024).

Dzurisin, Daniel (2007). *Volcano Deformation: Geodetic Monitoring Techniques*. Springer-Praxis Books in Geophysical Sciences. Berlin ; New York : Chichester, UK: Springer ; Praxis. 441 pp. ISBN: 978-3-540-42642-4.

Feppon, F. et al. (Sept. 15, 2020). "Topology Optimization of Thermal Fluid–Structure Systems Using Body-Fitted Meshes and Parallel Computing". In: *Journal of Computational Physics* 417, p. 109574. ISSN: 0021-9991. DOI: 10.1016/j.jcp.2020.109574. URL: https://www.sciencedirect.com/science/article/pii/S002199912030348X (visited on 08/22/2024).

Frei, Walter (Dec. 29, 2015). *Designing New Structures with Shape Optimization*. COMSOL. URL: https://www.comsol.com/blogs/designing-new-structures-with-shape-optimization (visited on 08/22/2024).

Geuzaine, Christophe, Jean-Francois Remacle, and P Dular (2009). "Gmsh: A Three-Dimensional Finite Element Mesh Generator". In: *International Journal for Numerical Methods in Engineering* 79.11, pp. 1309–1331.

Greiner, Sonja HM (2021). "Including Topography and a 3D-elastic Structure into a Finite-Element Deformation Model of Grímsvötn, Iceland". PhD thesis. URL: http://hdl.handle.net/1946/38435.

Hadamard, J. (1908). *Mémoire Sur Le Problème d'analyse Relatif a l'équilibre Des Plaques Élastiques Encastrèes*. Académie Des Sciences. Mémoires. Imprimerie nationale. URL: https://books.google.co.ma/books?id=8wSUmAEACAAJ.

Hecht, F. (2012). "New Development in FreeFem++". In: *Journal of Numerical Mathematics* 20.3-4, pp. 251–265. ISSN: 1570-2820. URL: https://freefem.org/.

Hickey, James and Joachim Gottsmann (June 2014). "Benchmarking and Developing Numerical Finite Element Models of Volcanic Deformation". In: *Journal of Volcanology and Geothermal Research* 280, pp. 126–130. ISSN: 03770273. DOI: 10.1016/j.jvolgeores.2014.05.011. URL: https://linkinghub.elsevier.com/retrieve/pii/S037702731400153X (visited on 02/29/2024).

Hunter, William et al. (2017). *ToPy - Topology Optimization with Python*. GitHub. URL: https://github.com/williamhunter/topy.

Íslands, Landmælingar (2024). *ISN2016 - Tækniskýrsla*. Landmælingar Íslands. URL: https://www.lmi.is/is/um-lmi/frettayfirlit/isn2016-tkniskrsla (visited on 08/22/2024).

Le Quilliec, Guenhael (2014). “Topology Optimization Procedure TOPOPTIM and Other Various Developments Made with Cast3M”. In: DOI: 10.13140/2.1.2718.3682. URL: http://rgdoi.net//10.13140/2.1.2718.3682 (visited on 02/29/2024).

McTigue, D. F. (Nov. 10, 1987). “Elastic Stress and Deformation near a Finite Spherical Magma Body: Resolution of the Point Source Paradox”. In: *Journal of Geophysical Research: Solid Earth* 92.B12, pp. 12931–12940. ISSN: 0148-0227. DOI: 10.1029/JB092iB12p12931. URL: https://agupubs.onlinelibrary.wiley.com/doi/10.1029/JB092iB12p12931 (visited on 02/27/2024).

Mogi, Kiyoo (1958). “Relations between the Eruptions of Various Volcanoes and the Deformations of the Ground Surfaces around Them”. In: *Earthq Res Inst* 36, pp. 99–134.

Parks, Michelle et al. (Jan. 23, 2024). “Data and Geodetic Modelling Results for Science Article "Fracturing and Tectonic Stress Drives Ultra-Rapid Magma Flow into Dikes"”. In: URL: https://osf.io/9rcq7/ (visited on 08/21/2024).

Sigmund, O. (Apr. 1, 2001). “A 99 Line Topology Optimization Code Written in Matlab”. In: *Structural and Multidisciplinary Optimization* 21.2, pp. 120–127. ISSN: 1615-1488. DOI: 10.1007/s001580050176. URL: https://doi.org/10.1007/s001580050176 (visited on 08/22/2024).

Sigmund, Ole and Kurt Maute (Dec. 1, 2013). “Topology Optimization Approaches”. In: *Structural and Multidisciplinary Optimization* 48.6, pp. 1031–1055. ISSN: 1615-1488. DOI: 10.1007/s00158-013-0978-6. URL: https://doi.org/10.1007/s00158-013-0978-6 (visited on 08/21/2024).

Sigmundsson, Freysteinn et al. (Mar. 15, 2024). “Fracturing and Tectonic Stress Drive Ultrarapid Magma Flow into Dikes”. In: *Science* 383.6688, pp. 1228–1235. DOI: 10.1126/science.adn2838. URL: https://www.science.org/doi/10.1126/science.adn2838 (visited on 08/21/2024).

Slavov, Stoyan and Mariya Konsulova-Bakalova (Jan. 15, 2019). “Optimizing Weight of Housing Elements of Two-stage Reducer by Using the Topology Management Optimization Capabilities Integrated in SOLIDWORKS: A Case Study”. In: *Machines* 7.1, p. 9. ISSN: 2075-1702. DOI: 10.3390/machines7010009. URL: https://www.mdpi.com/2075-1702/7/1/9 (visited on 08/22/2024).

Taylor, Nicola C., Jessica H. Johnson, and Richard A. Herd (Nov. 1, 2021). “Making the Most of the Mogi Model: Size Matters”. In: *Journal of Volcanology and Geothermal Research* 419, p. 107380. ISSN: 0377-0273.

DOI: 10.1016/j.jvolgeores.2021.107380. URL: https://www.sciencedirect.com/science/article/pii/S0377027321002092 (visited on 08/22/2024).
Trasatti, Elisa (July 1, 2022). "Volcanic and Seismic Source Modeling: An Open Tool for Geodetic Data Modeling". In: *Frontiers in Earth Science* 10. ISSN: 2296-6463. DOI: 10.3389/feart.2022.917222. URL: https://www.frontiersin.org/journals/earth-science/articles/10.3389/feart.2022.917222/full (visited on 08/21/2024).
Velez, Maria Laura et al. (Apr. 30, 2011). "Deformation of Copahue Volcano: Inversion of InSAR Data Using a Genetic Algorithm". In: *Journal of Volcanology and Geothermal Research* 202.1, pp. 117–126. ISSN: 0377-0273. DOI: 10.1016/j.jvolgeores.2011.01.012. URL: https://www.sciencedirect.com/science/article/pii/S0377027311000394 (visited on 08/22/2024).
Yang, Xue-Min, Paul M. Davis, and James H. Dieterich (1988). "Deformation from Inflation of a Dipping Finite Prolate Spheroid in an Elastic Half-Space as a Model for Volcanic Stressing". In: *Journal of Geophysical Research: Solid Earth* 93.B5, pp. 4249–4257. ISSN: 2156-2202. DOI: 10.1029/JB093iB05p04249. URL: https://onlinelibrary.wiley.com/doi/abs/10.1029/JB093iB05p04249 (visited on 08/22/2024).